EVS24
Stavanger, Norway, May 13-16, 2009

Battery electric vehicles in low voltage grids – modelling and simulation of batteries within the system

Simon Schwunk, Matthias Vetter
Fraunhofer Institute for Solar Energy Systems ISE, Heidenhofstr. 2, D-79110 Freiburg,Germany
Tel +49 (0)761/4588-5219; Fax: +49(0)761/4588-9000; simon.schwunk@ise.fraunhofer.de

Abstract

Battery electric vehicles are discussed as a solution for future environmental and transportation problems. The storage technology mostly discussed is lithium-ion due to its high energy density and its high cycle and calendar life times. First the different kinds of available lithium-ion batteries are described. The electrode materials are discussed in detail while for the electrolytes they are just briefly mentioned. The main focus will be to model the batteries in the two system environments – the car and the low voltage grid. Detailed descriptions of the battery pack model, the components of the low voltage grid and driving profiles are given. Simulation results will give a first idea of the impacts of different operating strategies: first operation only for transportation, second as storage during times of high renewable energy production and third operation also for storing renewable energy for feeding back energy in times with high demand in low voltage grids. The results show a need for intelligent operating strategies, while showing that the use of the vehicles as storages for renewable energies can be problematic due to ageing effects.

Keywords: lithium battery, modelling, simulation, vehicle to grid, energy storage

1 Introduction

The increasing share of renewable energies in the electricity grids causes a need for storage because of capacities and fluctuating energy production [1]. Since storing energy always means high cost [2,3,4] one has to maximize the advantages of the storage. At the moment there are activities to reduce the dependence from oil by electric mobility, battery electric vehicles or also plug-in hybrid cars. Because statistically cars are needed less than one hour per day in Germany in the range of 30 to 60 km [5,25,26,27] - though the sources are not clear about the exact times and distances - the batteries can also be used as storage for renewable energies, e.g. for wind energy during night time and photovoltaics during day time. The stored energy can then be used during times of high demand. From a technical point of view one has to secure the mobility needs of the car user, when using the car batteries also as storages for the grid. In such a scenario the expensive batteries are used for stationary and mobile purposes, which could reduce the overall investment costs significantly, if the right incentives are given. But one has to take the higher stress for the batteries into account, which can cause earlier ageing.

For determining the advantages and disadvantages simulations are needed. The system simulator employed for producing the results of this paper is Dymola [6] using the object-oriented modelling language Modelica [7]. This provides a quick, but consistent implementation of models with high reusability of models afterwards.

2 Battery technologies

Today's commercially available lithium-ion secondary batteries typically consist of an anode made of carbon, mostly graphite, and a cathode consisting of a $LiMO_2$. M stands for a transition metal [8]. The electrolyte consists of an organic solvent like propylene carbonate, ethylene carbonate, dimethyl sulfoxide and others. As conducting salts $LiPF_6$, $LiBF_4$, $LiClO_4$, $LiAsF_6$ or others are dissolved within the electrolyte [9, 10]. The charging process on the cathode can be described by following equation:

$$LiMO_2 \rightarrow Li_{1-x}MO_2 + xLi^+ + xe^- \quad (1)$$

The charging process on the anode can be described by following equation:

$$C + xLi^+ + xe^- \rightarrow Li_xC \quad (2)$$

The main advantages of today's lithium-ion batteries are high voltage, since lithium is the most electronegative element, high volumetric and gravimetric energy density, good cycle and shelf life, quick charging and a low self-discharge rate [9].

Due to the intercalation processes in the electrodes, the formation of a so called SEI (solid electrolyte interface) layer on the anode and other factors high cycle life can be achieved. The SEI layer is formed during the first cycle due to decomposition of the electrolyte.

Depending on the material of the electrodes the lithium-ion batteries differ substantially in voltage levels, energy and power densities and ageing characteristics. An example for the difference in voltage levels between two important cathode materials is given in Figure 1.

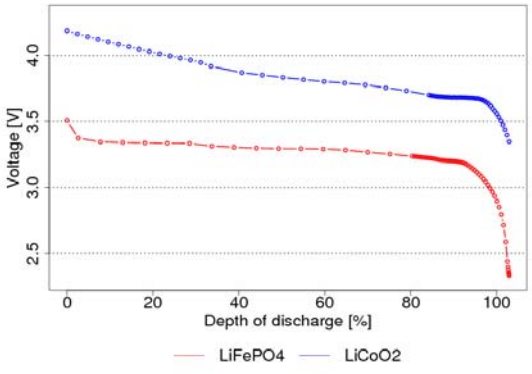

Figure 1: Open circuit voltage of a conventional $LiCoO_2$/graphite battery and a $LiFePO_4$/graphite battery.

2.1 Cathodes

The most commonly used cathode material today is $LiCoO_2$. Sony introduced those batteries in 1991 [9], and since then they found a large application area in consumer products like mobile phones and laptops. The material has a layered structure, high capacity with 150 $mAhg^{-1}$ (theoretically 248 $mAhg^{-1}$) [15] and good cylclability [8, 9]. Despite the good experiences in consumer products batteries made of this material are not of interest for electric vehicle applications due to several reasons: First of all cobalt is an expensive raw material contributing substantially to the costs of a lithium-ion battery making it economically unattractive. Second the tolerance towards thermal, mechanical or electrical abuse is low. Internal or external short circuits or thermal heating can lead to an exothermic reaction making accumulators burn as it could be seen for laptop batteries in the last years.

There are some other materials available which promise to be more suitable for electric vehicle applications. Nickel can be used instead of cobalt because it is isostructural. But a pure $LiNiO_2$ is difficult to synthesize and also suffers from a rapid decrease in capacity [11, 9]. Thus it is combined with cobalt to $LiNi_{1-x}Co_xO_2$ [11], which is offered by different companies today as high energy cell with high capacities. By doping this material with aluminium or magnesium the composition is very stable in the discharged state and can even stand elevated temperatures [11]. Another mixture of different materials combining good characteristics is $LiNi_{1/3}Co_{1/3}Mn_{1/3}O_2$ called NMC [12].

Overall they have an excellent cycle life, if the end of charge voltage of normally 4.2 V is not exceeded. A reduction of the end of charge voltage to 4.1 V can increase cycle life even further. A problem that remains is the exothermic reaction occurring at very high temperatures. This means a safety risk, if those cells are abused.

A material that does not show that dangerous characteristics at high temperatures and is also rather cheap is $LiMn_2O_4$. The material has a spinel structure. Though the safety advantages are significant it suffers from several drawbacks: lower discharge capacity than $LiCoO_2$ and problems with cyclabilty [9]. Especially the last characteristic does not make the material the first choice for electric vehicle applications.

A new and very promising candidate is $LiFePO_4$. The material is said to be safe and environmentally acceptable [8]. Though the capacity is just around 160 $mAhg^{-1}$[8], this could be sufficient in the application still. $LiFePO_4$ cells have a nominal voltage of 3.3 V. The charging and discharging curves are extremely flat causing problems when determining the state of charge. What makes it

very suitable for the application is the very high cyclabilty. Excellent life times for this material can be expected if it is handled carefully [8].
At the moment researchers are working on $LiVPO_4F$ and $Li_3V_2(PO_4)_3$ which have similar properties as $LiFePO_4$, but higher voltages [13].

2.2 Anodes

The most common anode material today is carbon, mostly used as graphite, which has a maximum charge capacity up to 372 $mAhg^{-1}$. The carbon electrode operates out of the stability window of the electrolyte, which leads to a decomposition of the electrolyte on the surface of the carbon anode. This leads to a significant capacity loss during the first formation cycles. Afterwards the SEI layer remains quite stable and good cycle performance can be achieved despite the potential of the carbon [11, 14].
For increasing the capacity of the anode further, intensive work is done on analysing silicon as anode material. The potential versus Li/Li+ is similar to that of carbon but the achievable capacity is a magnitude higher than that of carbon [15]. But these anode materials have not come close to a product yet.
A material discussed among researchers today and already available in some products is lithium titanate. This material has a rather high potential versus Li/Li+, which leads to the fact, that it is operated within the stability window of the electrolyte. This will increase the life time and power density of the batteries. Additionally it is assumed to be a safe material. But the high potential of the material is causing a reduced cell voltage, thus reducing the energy density drastically [15]. Therefore it is more interesting for hybrid vehicles than for electric vehicles and plug-in hybrids with a substantial driving range.

3 System modelling

For simulating a low voltage grid with photovoltaic generators, consumers and vehicles used as distributed storages extensive modelling is necessary. One must reproduce the cabling, the middle voltage grid, the consumption the behaviour of the storages and the driving profiles accurately. Simultaneously calculation times must remain on an acceptable level. Therefore e.g. phasor description for the electric components was chosen and implemented [16].
As storages $LiFePO_4$/graphite battery packs with a total capacity of 16 kWh per vehicle was taken as a basis. Overall there are 70 cars within the grid. During day time of course there is just a part of them connected to the low voltage grid. The other cars are assumed to have comparable current profiles at work for example.
The low voltage grid contains about 100 households. The photovoltaic generator has an overall peak power of 200 kW_p.

3.1 Low voltage grid

The analysed test grid is highly intermeshed and redundant. It is supplied from a 20 kV middle voltage grid via a 400 kVA transformer. But the middle voltage grid is mostly at a voltage level of 20.3 kV

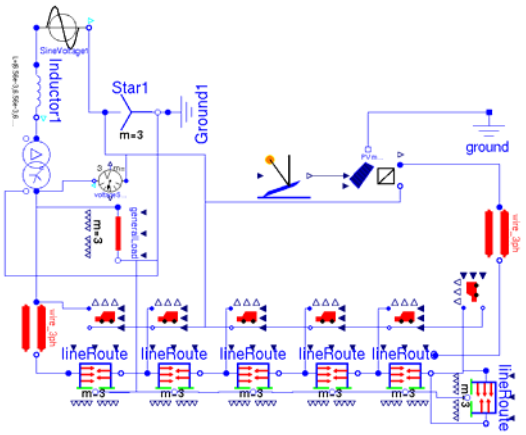

Figure 2: Dymola model of the low voltage grid with distributed electric vehicles as storages.

The transformer is the only connecting point between the low voltage and the middle voltage grid. Therefore the middle voltage grid can be reproduced via an equivalent two terminal network consisting of an ideal voltage source and an impedance. For high and low voltage grids the ohmic part of the impedance can be neglected. So the reactance X_Q is calculated from the grid voltage V_{nN} and the short circuit power S_k'' [17]:

$$X_Q = \frac{1.1 \cdot V_{nN}^2}{S_k''} \qquad (3)$$

The cable model used corresponds to the common model in electrical engineering. Short cables like here in the low voltage grid are reproduced as π- or T-quadrupole. Here a π-quadrupole is displayed in Figure 3.

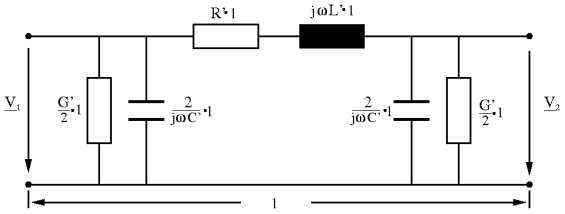

Figure 3: Eqivalent quadripole for cables.

The cable is then characterised by the resistance load per unit length R', inductance load per unit length L', conductance load per unit length G' and capacitance load per unit length C'. For low voltage grids the capacitance and the conductance can be neglected. For accelerating the simulation this model reduction was done.
The cable is made of aluminium and its type designation is NAYY 4x150SE 0.6/1kV. For the photovoltaic generator a copper cable with the type designation NYY 4x95SM 0.6/1kV was used.

3.2 Photovoltaic generator

A Modelica [7] model based on the 2 diodes model was implemented. This is the standard model for describing the behaviour of a solar cell as exactly as possible [18, 19]. The two diodes describe different recombination mechanisms while the parallel resistance describes currents flowing at grain boundaries and the shunt resistance describes all resistances in the cell like current collectors and conductivity of charge carriers in the semiconductor. The current source describes the charge carriers produced by the absorbed photons. The model is displayed in Figure 4.

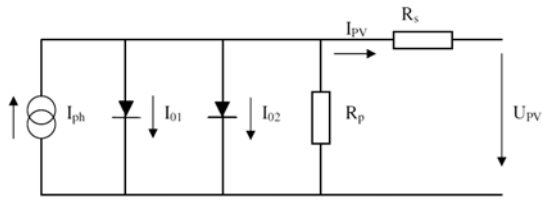

Figure 4: Two diodes model for exact simulation of photovoltaic cell.

Since solar cells produce DC current this must be converted into AC current for being able to feed into the grid. An inverter is necessary.
The model is displayed in Figure 5. A MPP tracker controls voltage and current of the solar cells in a way that it gets the maximum power from the cells. This point is called the maximum power point (MPP). This power is fed through a efficiency characteristic determining the AC power output. Afterwards the current fed into the grid is determined from the AC power and the grid voltage assuming a phase shifting cos φ to be zero as it is for solar inverters today.
For modelling the inverter the efficiency characteristic of a highly efficient inverter was fitted. The efficiency is high over a wide range of input power guaranteeing a high efficiency also in times of low irradiation.

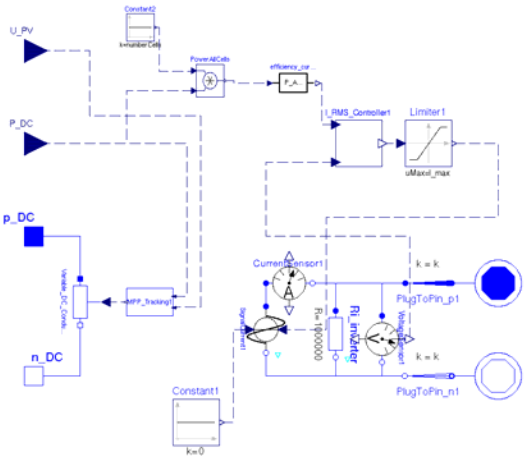

Figure 5: Modelica model of a photovoltaic inverter with MPP tracking.

The output power and the maximum power point also change with temperature and irradiance. Thus it is not sufficient to just fix a certain voltage but one has to adapt the voltage of the solar cells according to the operating conditions.
The MPP tracking algorithm uses a gradient based method [19]. The power of a solar cell increases first the voltage, until the maximum power point is reached and then falls again like it is displayed in Figure 6.
Therefore the algorithm increases the voltage as long as power increases. As soon as the power decreases, while voltage is increased, the algorithm decreases the voltage.
The accuracy of the algorithm is depending on the increase in voltage the algorithm performs and on the sampling time. Also it does not determine a stable working point, but it still changes the working point slightly also under stable operating conditions as can be seen in Figure 6. As no shading is assumed in the model, this algorithm is fully sufficient for the purpose of this study. How to extent the algorithm for making it work under more complicated working conditions is described in [19].

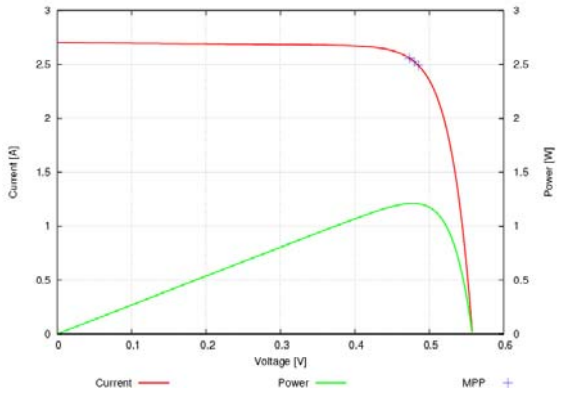

Figure 6: Electrical behaviour of a solar cell. Displayed are voltage, current and working points of the tracking algorithm.

The algorithm was first implemented in Modelica code and afterwards implemented in Ansi-C and included via an external interface for speeding up simulation time. Thus if another control algorithm from a real inverter should be tried out this can be easily done by exchanging the ANSI-C code.

3.3 Battery pack

For simulating a battery pack first the battery cell was modelled and then an up scaling was done, which avoided a huge increase in calculation time while not neglecting effects like additional losses due to charge balancing, monitoring electronics and cooling. While the cell model could be validated, the pack model could not be validated with real measurement data, since battery packs in this size are not easily available.

3.3.1 Battery cell model

Shepherd proposed a model in [29] that is suitable for constant discharge currents and suggested that it would also be suitable for constant charge currents. In [30] the so called Hyman equation, a different formulation of the Shepherd equation, was used for the simulation of lead acid batteries. The model has the advantage of being relatively easy to parameterise and having little parameters to be determined. In [23,24] the model was adapted for lithium-ion batteries.

All parameters and variables for this chapter are described in Table 1. The changing variables in the Hyman formulation are voltage U, current I, depth of discharge DOD, and state of charge SOC. The charging equation was modified slightly according to [23,24] for obtaining better simulation results.

The discharging process is described by the equation below:

$$U = U_{0d} - g_d \cdot DOD + \rho_d \cdot \frac{I}{Q_N} \cdot (1 + M_d \cdot \frac{DOD}{C_d - DOD}) + A_d \cdot e^{-(v_d \cdot I + w_d) DOD} \quad (4)$$

The charging process is described by the equation below:

$$U = U_c - g_c \cdot DOD + \rho_c \cdot \frac{I}{Q_N} \cdot + M_c \cdot \frac{\rho_c}{Q_N} \cdot \frac{DOD}{C_c - DOD} + A_c \cdot e^{-(v_c \cdot I + w_c) DOD} \quad (5)$$

Two important variables still have to be defined now: SOC and DOD. The state of charge SOC is determined as the integral of the battery current I minus the loss current I_{loss}. Since the charge factor of lithium-ion batteries is one, I_{loss} is neglected. The starting value of the state of charge SOC_0 must be known. This is formulated in the equation below:

$$SOC = SOC_0 + \frac{1}{Q_N} \int Idt \quad (6)$$

$$DOD = 1 - SOC \quad (7)$$

Table 1: Variables and parameters used for the modified Shepherd model [23,24].

Parameter	Unit	Description
U_0	V	Open circuit voltage
ρ_i	Ω Ah	Parameter of ohmic resistances
M_i	-	Coefficient for charge transfer overpotential
g_i	V	Coefficient for ion concentration
C_i	-	Capacity coefficient
Q_N	Ah	Nominal capacity (C_{10})
A_i	V	Starting voltage of exponential term
v_i	1/A	Current dependent exponential coefficient
w_i	-	Current independent exponential coefficient
i	-	Distinction between charge (c) and discharge (d) parameters
SOC	-	State of charge of the battery
SOC_0	-	Starting value for the state of charge of the battery
DOD	-	Depth of discharge

A test profile was defined for validation purposes. The profile covers all states of charge during

simulation and changes several times between different charging and discharging currents. At one point the battery is discharged completely. The profile can be seen in figure 7.
Of special interest were the errors occurring at very high and very low states of charge, dynamic current profiles, phases with no current and changes between charge and discharge. As one can see in figure 7 the highest errors occur at a very low state of charge, especially when the current is zero. The relative percentage error (RPE) even exceeds 60 % for a short time. There are two reasons for that. First the dynamics are not modelled and the relaxation time of lithium ion batteries is high in low states of charge. Before the current was applied again, the error had already fallen to about ten percent and kept on falling. Second the Shepherd equation is unable to model the open circuit voltage at low state of charge correctly as it is shown in figure 1.
The first and the second term of the equations 5 and 6 are completely independent from the current. The exponential term described in the equations 3 and 4 is at least partially current independent. But the third term responsible for the quick fall at the end of discharge is completely current dependent and zero if the current is zero. Thus at the end of discharge the model can just show linear behaviour though the battery behaviour is highly non-linear.
Hence at low states of charge the error is significant and could not be reduced easily just by a better optimisation.
If the battery is in rest states of charge above 10 % the open circuit voltage is reproduced well by the Shepherd model. The dynamics of the voltages are not represented by the model, but the error still remains on a very acceptable level. The changes between the charge and discharge equation are of course discontinuous, but the error remains low.
Since the relative error remains well below 2 % the model is very well suitable for our application. The voltage is very well produced in all phases with a state of charge above 10 %. The average error is 3.1 %. Therefore one can conclude that the model is applicable for our simulation purposes.

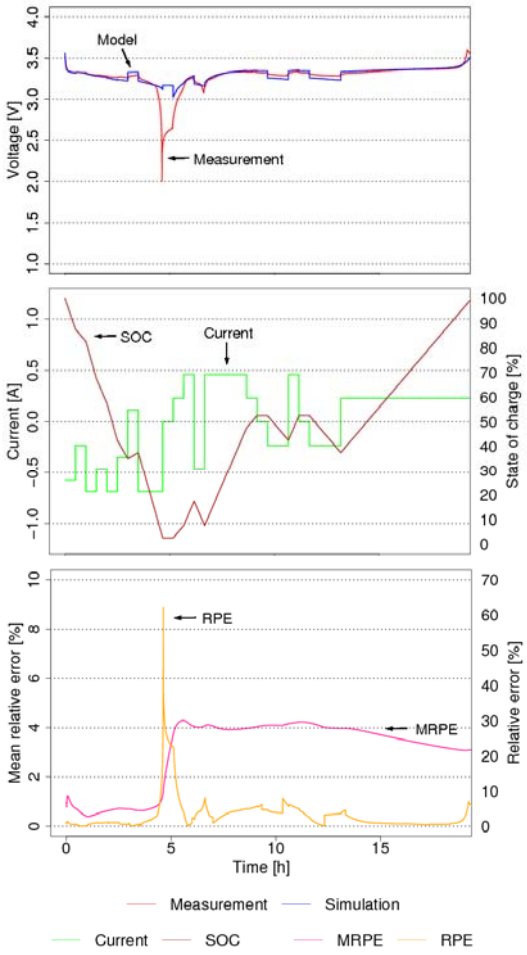

Figure 7: Validation sequence for model of a lithium iron phosphate battery. On top the voltage is displayed in the middle the current and the state of charge, at the bottom the mean relative error and the relative error.

3.3.2 Up scaling to the pack level

While for simulating cell behaviour a huge amount of papers is available, there are a lot less for simulating battery packs, especially if it comes to lithium-ion batteries. In [21] a pack model is introduced, that only varies two important parameters in the cells and keeps the rest of the cell model stable. Thus parameterisation effort is significantly reduced while still being able to accurately model the behaviour of the cells. Calculation time will remain high since still single cells are simulated. This will be very important if the exact capacity and the power capability of the pack are in the focus. Here the amount of energy that can be drawn from a pack and the general voltage and current characteristics were of interest. Thus such a detailed model is not necessary.
For getting the correct voltage and current values, the results from the cell are up scaled with the

number of cells in a row and the number of cells in parallel.

$$V_{batt} = V_{cell} \cdot n_{series} \quad (8)$$

$$I_{batt} = I_{cell} \cdot n_{parallel} \quad (9)$$

Since there are additional losses due to cell balancing and the electronics for the battery pack and cooling, loss factors are introduced. First the charging efficiency is decreased by I_{loss}:

$$SOC = SOC_0 + \frac{1}{Q_N} \int I - I_{loss} dt \quad (10)$$

Second the amount of power charged into the battery is decreased:

$$P_{loss} = \eta_{loss} \cdot P_{charge} \quad (11)$$

3.4 Vehicle profiles

Since real velocity profiles are not available easily there are no power profiles determining how much power the car needs on the road. Based on the NEDC [22] an assumption for the power needed for electric driving was made. The kinetic power a car needs is determined by the acceleration, the rolling resistance and the aerodynamic resistance:

$$P_{car} = P_{acc} + P_{roll} + P_{air} \quad (12)$$

In conventional cars the accelerating power can only be positive because the energy consumed during braking could not be regained. For electric vehicles the power during braking becomes negative. The energy stored in a moving mass is given by:

$$E_{kin} = \frac{1}{2} m v^2 \quad (13)$$

The power for acceleration is then given by its derivative.

$$P_{acc} = \frac{dE_{kin}}{dt} \quad (14)$$

The rolling resistance is calculated by the rolling resistance coefficient and the normal force. Though the rolling resistance coefficient is depending on the velocity and the contact force, this is neglected here. The work used in this case is then calculated by

$$W_{roll} = F_{roll} \cdot s \quad (15)$$

Again the derivative is taken to determine the power.

$$P_{roll} = \frac{dW_{roll}}{dt} \quad (16)$$

The aerodynamic force depends on the area, the air drag coefficient, the air density and the velocity:

$$F_{air} = A \cdot c_W \cdot \rho / 2 \cdot v^2 \quad (17)$$

Therefore the work needed to overcome the aerodynamic resistance is calculated as follows:

$$W_{air} = F_{air} \cdot s \quad (18)$$

The derivative of the work is equal to the power.

$$P_{air} = \frac{dW_{air}}{dt} \quad (19)$$

The losses caused by the inverter and the electric motor are calculated as constant loss factors.

The urban and the interurban NEDC parts are set together to a 20 min and 18 km mixed profile and a purely urban 10 min and 6 km profile. Both profiles are driven two times a day each.

3.5 Household profiles

The electric consumers in the analysed grid are only private households. If one excludes the electricity for electric mobility the peak power is roundabout 125 kW. The consumption profiles are taken from a load profile from the utility Vattenfall and have hourly average values. The profile is called GH0 and is based on the VDEW H0 profile, which is the standard profile for households [28].

The overall consumption in one year was estimated on the basis of an average of 4.5 persons per household with 101 accommodation units. As average consumption of 1110 kWh per capita for a four persons household is given in [20], which is assumed to be the same for a household with 4.5 persons.

4 Simulation results

Within simulations the possibilities in the grid for smoothing the load profile and the effects of different operating strategies for the mobile storages were analysed.

In scenario 1 all vehicles are recharged immediately with 3 kW as soon as they are connected to the grid for always guaranteeing the maximum driving range. In scenario 2 the vehicles are used as shiftable loads within the grid and are recharged during times of high production of photovoltaic energy with different power levels. The aim was to minimize the electricity demand from the middle voltage grid and to consume the electricity produced by the photovoltaic locally. In scenario number three the vehicles are also able to feed back energy into the grid. The evening peak is reduced to a maximum of 50 kW.

4.1 Battery pack

First the battery pack is analysed. Figure 8 shows simulation results from a 20 min drive – urban and interurban adding up to about 18 km of driving. The graph on top shows voltage and current. As one can see the currents change rapidly and though the battery is quite big with 16 kWh, still current peaks of more than two and a half times the capacity occur.

Due to neglecting capacitive effects only the stationary voltages are reproduced. Since not the power limitations are in the focus of the paper, but the energy that can be stored within the battery this is fully sufficient.

The driving profile here is a mixed urban / interurban profile. Significant recuperation can only be seen during urban driving while the battery is quickly discharged during the interurban part due to the higher velocities.

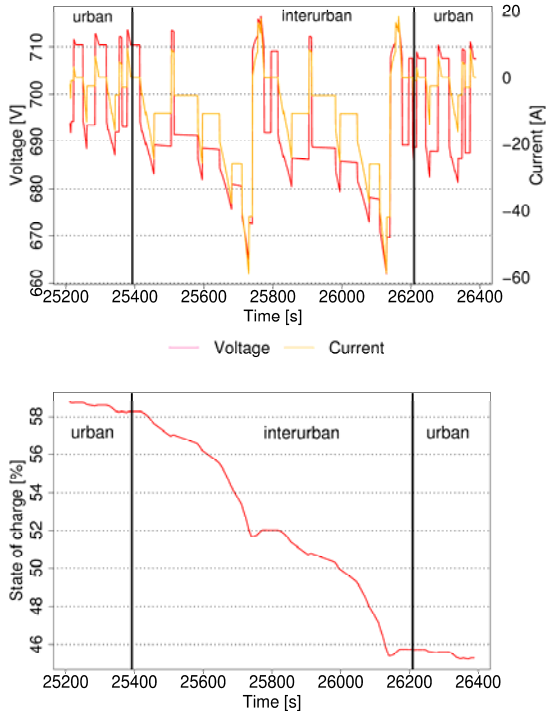

Figure 8: Simulation results of the battery pack during driving. On top the current and the voltage are displayed, at the bottom the state of charge during driving.

In the first scenario the operation strategy tries to immediately recharge the battery. Therefore the battery is often in full state of charge. In the two other scenarios the batteries are only recharged moderately during night times, the full charge is done from photovoltaic energy during day time. Late in the evening they are not charged due to the high evening peak in electricity consumption. In scenario 3 the vehicles are even feeding energy back into the grid at that time of the day with a power of 300 W per vehicle. Thus the states of charge of the batteries in these scenarios are more in the middle range.

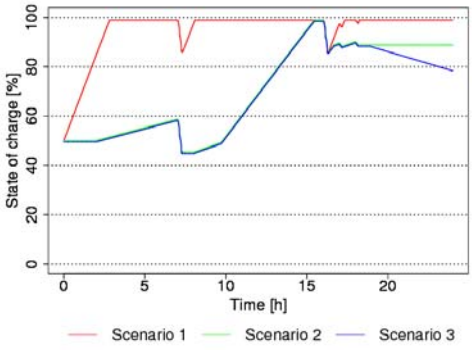

Figure 9: States of charge for the three different scenarios during the day. Scenario 1 describes immediate recharge. Scenario 2 uses the storages as shiftable loads, while scenario 3 also does peak shaving in the evening.

In table 2 efficiency, Ah turnovers and the difference in the states of charge of the batteries between the start and the end of the day ΔSOC are displayed. The overall efficiency of the battery pack is relatively high above 90 %. The Ah turnover in scenario 1 is higher than in scenario 2. The reason for this is the rather low state of charge of the batteries at the beginning of the day. Therefore more energy must be charged into the battery in scenario 1 because it should be always as full as possible. This is not the way in scenario 2 because the battery is recharged, when it is suitable to the grid. Therefore the battery is not as full as in scenario 1. This effect on Ah turnover should not be seen after several days, since the energy demand of the cars is the same in both scenarios.

In scenario three the charge turnover increases by 5.9 % compared to scenario 2 while the state of charge is 6 % lower at the same time. The peak shaving in the evening increases the charge turnvover in this scenario about 11 % in comparison to scenario 2. Since charge turnover is an important factor for the ageing mechanisms in the battery, this will lead to a decreased life time of the battery. The exact decrease also depends on other ageing factors interacting with this one.

Table 2: Results for the battery pack in the three different scenarios. The efficiency, the Ah turnovers and the difference in the state of charge between the start and the end of the day is given below.

Scenario	Immediate recharge	Dispatchable load	Peak shaving
Efficiency	0.908	0.907	0.902
Ah turnover	26.2	23.9	26.2
Ah from grid	18.3	15.9	16.0
Ah to grid	0	0	2.2
ΔSOC	0.49	0.39	0.29

4.2 Energy fluxes in the grid

The energy fluxes for the calculated scenarios differ significantly as can be seen from Figure 10. Displayed are the energy fluxes at the transformer, the photovoltaic generator, the households and the cars. In scenario 1 one can see that already a simultaneous immediate recharge of all cars with 3 kW can lead to a multiple of the original peak power, even during times with low demand. Depending on the statistical distribution of charging strong restrictions for the users can be necessary to secure the electricity supply.

An intelligent operating control strategy in the case of big photovoltaic production like in scenario 2 can prevent the energy from being fed into the middle voltage grid, but make the batteries in the cars being charged. Therefore the energy fluxes at the transformer are smoothed.

In scenario 3 70 cars feed back 300 W into the grid in the evening. Thus the evening peak is reduced about 30 %. On the other hand the Ah turnover increases quickly as described in section 4.1. The possibilities of using the vehicles as energy storages seem to be limited, while putting severe stress on the battery.

The voltage levels were not affected in a significant way in these calculations since an over dimensioned, but real grid was simulated like it is described in [31]. In other grid topologies also in Germany, but especially in countries with less dense population or worse infrastructure scenarios like these could already cause problems.

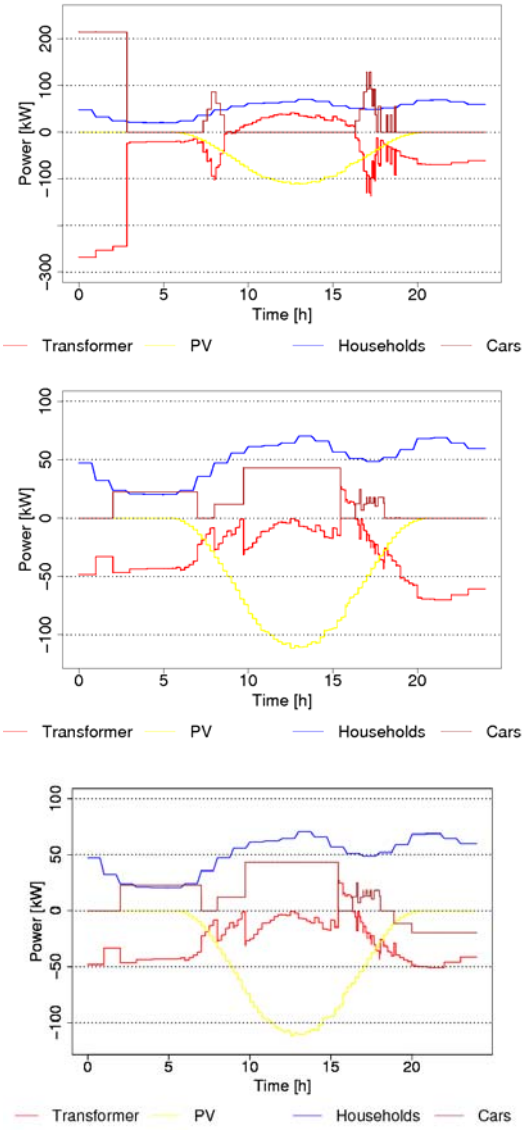

Figure 10: Energy fluxes in the middle voltage grid for the three different scenarios. On top the scenario with immediate recharge, in the middle the shiftable load scenario, at bottom the peak shaving scenario.

5 Conclusions

A method for modelling, simulating and analysing questions about plug in hybrid or battery electric vehicles, especially in big systems, was introduced. Models implemented in Modelica for the low voltage grid and the components as well as the battery pack in the vehicle environment are described. The modelling depth is a compromise between calculation times, parameterisation effort and accuracy.

First simulation results lead to following conclusions: First of all an intelligent operating control strategy taking all energy fluxes in the low

voltage grid into account seems to be necessary for avoiding unreasonably high power peaks in the low voltage grid. If one uses the storages in the vehicles not just as shiftable loads but also as storages feeding back into the grid, this leads to a significant increase in charge turnover. Additionally one has to take the other ageing factors into account; therefore an accurate ageing model of the battery is needed for determining and quantifying the harming effects on the battery caused by the use as storage. Despite some drawbacks a first hint on the problem caused by the dual use of such a battery is given.
Compensation schemes for the owners of the batteries or a leasing model, in which the car driver leases a battery from his utility, could be an economic solution for such a problem. For finding a suitable business model for the future more quantifiable knowledge about the ageing effects within the battery must be acquired and more detailed simulation studies, based on the method given in this paper, must be carried out.

Acknowledgments

The work was carried out within the Project EMSIS with the support code 01SF0708 for German French cooperation between Fraunhofer and Carnot institutes. The project was financed by the German Ministry of Education and Research.

References

[1] Deutsche Energieagentur GmbH (dena): Energiewirtschaftliche Planung für die Netzintegration von Windenergie in Deutschland an Land und Offshore bis zum Jahr 2020, www.dena.de, 2005

[2] Sauer, D.U.: Detailed cost calculations for stationary battery storage systems, Second International Renewable Energy Storage Conference (IRESII), Bonn, 2007

[3] Sauer, D.U.: Detailed cost calculations for stationary battery storage systems, Third International Renewable Energy Storage Conference (IRESIII), Berlin, 2008

[4] Sauer, D.U. et al.: Energy storage technologies for grids with high penetration of renewable energies and for grid connected PV systems, 23rd European Photovoltaic Solar Energy Conference, Valencia, 2008

[5] Podewils, Ch.: Organisierte Verschwendung, Photon, pp. 28- 35, April 2007

[6] Dymola, www.dymola.de, accessed on March, 25th 2009

[7] Fritzson, P.: Principles of object-oriented modeling and simulation with Modelica 2.1, IEEE Press, Wiley-Interscience, 2004

[8] J. Goodenough, Cathode materials: A personal perspective, Journal of Power Sources 174 (2007) 996-1000

[9] Y. Nishi, Lithium ion secondary batteries; past 10 years and the future, Journal of Power Sources 100 (2001) 101-106

[10] K. Asakura et al., Study of life evaluation methods for Li-ion batteries for backup applications, Journal of Power Sources 119-121 (2003) 902-905

[11] J. Vetter et al., Ageing mechanisms in lithium-ion batteries, Journal of Power Sources 147 (2005) 269-281

[12] T. Ohzuku et al., An overview of positive-electrode materials for advanced lithium-ion batteries, Journal of Power Sources 174 (2007) 449-456

[13] H. Huang et al., Lithium metal phosphates, power and automotive application, Journal of Power Sources (2007), doi:10.1016/j.jpowsour.2008.08.024

[14] W.A. Schalkwijk and B Scrosati, Advances in Lithium-Ion Batteries, Kluwer Academic / Plenum Publishers New York, 2002

[15] M. Wohlfahrt-Mehrens, Material Aspects on Safety of Li-Ion Batteries, Presentation at 11th UECT - Ulmer ElectroChemical Talks Battery Tutorial, Ulm, 2008

[16] Enge, O.; Clauß, C.; Schneider, P.; Schwarz, P.; Vetter, M.; Schwunk, S.: Quasi-stationary AC analysis using phasor description with Modelica. 5th Int. Modelica Conference, Vienna, September 04-05, 2006, pp. 436-443

[17] Klaus Heuck; Klaus-Dieter Dettmann: Elektrische Energieversorgung, Vieweg-Verlag, 2005

[18] Würfel, P.: Physik der Solarzelle, Spektrum Akademischer Verlag, 2000

[19] Quaschning, V.: Regenerative Energiesysteme, Hanser Verlag, 2006

[20] VDEW: Privater Stromverbrauch, www.strom.de accessed on 24th January, 2005

[21] Dubarry, M. et al.:From single cell model to battery pack simulation for Li-ion batteries, Journal of Power sources (2008), doi:10.1016/j.jpowsour.2008.10.051

[22] Amtsblatt der Europäischen Union, Regelung Nr. 101 der Wirtschaftskommision der Vereinigten Staaten für Europa, 19.6.2007

[23] Simon Schwunk, Andreas Rudolph, Robert Thomas, Georg Bopp, Matthias Vetter: Lithium-ion secondary batteries for solar applications – characterisation and modelling, 3rd International Renewable Energy Storage Conference Berlin, 2008

[24] A. Rudolph, Modellierung der elektrischen Charak-teristik von Lithium-Ionen-Batterien, Diplomarbeit Fraunhofer ISE und HS Mannheim, 2008

[25] Sauer, D.U.: Stromspeicher in Netzen mit hohem Anteil erneuerbaren Energien, 23. Symposium Photovoltaische Solarenergie, Bad Staffelstein, March 5th to 7th, 2008

[26] City Darmstadt: http://www.darmstadt.de/wirtschaft/verkehr/parken/index.html, accessed on March 31st 2009

[27] Statistisches Bundesamt: Verkehr in Deutschland, www.destatis.de accessed on March 31st 2009

[28] VDI: Lastprofile in der leitungsgebundenen Energieversorgung VDI-GET Experten-seminar, Berlin, 24.4.2005.

[29] C.M. Shepherd; Design of Primary and Secondary Cells; J. Electrochem. Soc. 112 (1965) 657-664

[30] J. Schumacher; Digitale Simulation regenerativer elektrischer Energieversor-gungssysteme; Dissertation Universität Oldenburg 1991

[31] M. Thoma, Optimierte Betriebsführung von Niederspannungsnetzen mit einem hohen Anteil an dezentraler Erzeugung, Dissertation ETH Zürich, 2007

Authors

Simon Schwunk, M.Sc., Electrical Engineer. Electrical Engineering at the University of Applied Sciences Mannheim, finished in 2006 with Dipl-Ing. (FH). Electrical engineering at University of Hagen, finished with M.Sc. in 2008. Main fields of work: Modelling and simulation of batteries, monitoring and control algorithms for batteries, system analysis, concepts of plug in vehicles within smart grids, simulation and control of hybrid PV systems.

Dr.-Ing. Matthias Vetter, Electrical Engineer. PhD thesis in the field of modelling and development of control strategies for fuel cell systems. Until 2005 project manager in the field of modelling, simulation and development of control strategies for distributed power generation systems. Since 2005 head of group “Off-grid Power Supply” at Fraunhofer ISE. Work topics among others: Development and optimisation of battery management systems as well as supervisory control strategies and energy management systems for hybrid PV systems and electric vehiclesS.